
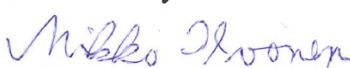





# The COOLOCE particle bed coolability experiments with a conical geometry: Test series 6 and 7

Authors: Eveliina Takasuo, Tuomo Kinnunen, Pekka H. Pankakoski, Stefan Holmström

Confidentiality: Public

|  |  |
|--|--|
| Report's title<br>The COOLOCE particle bed coolability experiments with a conical geometry: Test series 6 and 7  |  |
| Customer, contact person, address<br>SAFIR2014 Finnish Research Programme on Nuclear Power Plant Safety  | Order reference<br>23/2011SAF  |
| Project name<br>Core Debris Coolability  | Project number/Short name<br>73669/COOLOCE   |
| Author(s)<br>Eveliina Takasuo, Tuomo Kinnunen, Pekka H. Pankakoski, Stefan Holmström   | Pages<br>26 p. / 2 appendices  |
| Keywords<br>core debris, particle bed, dryout, coolability experiments, COOLOCE facility   | Report identification code<br>VTT-R-07097-11   |
| Summary<br><br><p>The COOLOCE experiments aim at investigating the coolability of particle beds of different geometries. A porous particle bed consisting of core debris may be formed as a result of a core melt accident in a nuclear power plant. The main objective of the experiments is to compare the dryout power of conical (heap-like) and cylindrical particle bed geometries. The present experiments, test series 6 and 7, have been conducted using a conical test bed which allows multi-dimensional infiltration of coolant through the surface of the cone. The pressure level of the experiments ranged from 1 bar to 3 bar (abs.) and the measured dryout power was between 26 kW and 43 kW. The coolability of the conical test bed is compared to that of the cylindrical test bed (test series 3-5) and the results of the COOLOCE experiments are summarized.</p> |  |
| Confidentiality  | Public   |
| Espoo, 13.10.2011<br>Written by<br><br>Eveliina Takasuo<br>Research Scientist   | Reviewed by<br><br>Mikko Ilvonen<br>Team Leader |
| Accepted by<br><br>Timo Vanttola<br>Technology Manager  |  |
| VTT's contact address<br>PO Box 1000, 02044 VTT, Finland   |  |
| Distribution (customer and VTT)<br>SAFIR2014 Reference Group 5<br>VTT: Timo Vanttola, Kaisa Simola, Vesa Suolainen, Eija Karita Puska, Mikko Ilvonen, Ville Hovi, Jarto Niemi, TK5013  |  |
| <i>The use of the name of the VTT Technical Research Centre of Finland (VTT) in advertising or publication in part of this report is only permissible with written authorisation from the VTT Technical Research Centre of Finland.</i>  |  |

## Contents

|     |  |    |
|-----|--|----|
| 1   | Introduction.....  | 2  |
| 2   | The test facility.....   | 3  |
| 2.1 | The test procedure.....  | 6  |
| 3   | Experimental results.....  | 8  |
| 3.1 | COOLOCE-6.....   | 8  |
| 3.2 | COOLOCE-7a, -7b and -7c.....   | 10 |
| 4   | Analysis.....  | 17 |
| 4.1 | Control power and calculated power.....  | 17 |
| 4.2 | Comparison of the conical and cylindrical bed results.....   | 19 |
| 4.3 | Comparison to the STYX experiments.....  | 22 |
| 5   | Discussion and summary.....  | 24 |
| 6   | Conclusions.....   | 25 |
|     | References.....  | 26 |
|     | APPENDIX A. Heater arrangement of the COOLOCE cylinder (top view of the pressure vessel bottom plate).....       | A1 |
|     | APPENDIX B. Thermocouple arrangement of the COOLOCE cylinder (top view of the pressure vessel bottom plate)..... | A2 |

## 1 Introduction

A porous particle bed – or debris bed - that consists of solidified corium may be formed as a result of a core melt accident in a nuclear power reactor. Depending on the design of the reactor, such a debris bed may be formed in the containment, e.g. in the flooded lower drywell of the Finnish BWR's after the failure of the reactor pressure vessel, or inside the pressure vessel. In order to ensure the coolability of the core debris and to prevent dryout and possible re-melting of the material, decay heat has to be removed from the material.

The COOLOCE test facility is used to investigate the coolability of porous particle beds of different geometries, focusing on ex-vessel cases. The main objective of the experimental programme is to compare the dryout power of a conical (heap-like) particle bed configuration to that of a cylindrical (evenly-distributed) top-flooded configuration. In addition to providing new data of the effect of particle bed geometry on coolability, the experimental results are used for code validation and development.

The present report describes the second series of experiments with a conical bed. The first set of experiments with a conical particle bed has been performed and reported earlier [1], [2]. Between the two series of conical bed experiments, a series of cylindrical bed tests was run [3]. The heating arrangement for the present conical bed experiments has been improved compared to the previous conical test set-up. The electrical heaters near the centre of the test bed have been changed to a model that has a more heat and corrosion resistant outer sheath than the original heaters. A built-in thermocouple is included in three of the heaters to monitor the heater sheath temperature. The aim of the modifications was to avoid the overheating problems encountered in the first experiments using the conical set-up [2].

The test series with the cylindrical set-up (COOLOCE-3–5) and the conical set-up (COOLOCE-6–7) along with the first experiments with the original conical set-up (COOLOCE-1–2) provide comparison data of the dryout behaviour of the two different geometries at the pressure range of 1 to 3 bars. In addition, pressure levels of 4 to 7 bars were reached with the cylindrical test bed. These results are useful for examining the pressure dependency of dryout and comparing the results to the results of the STYX experiments.

In addition to the description of the latest experiments, a brief analysis of the comparison of the two geometries is provided, as well as a discussion of the results concerning plant assessment. The results suggest that the coolability of the conical configuration is reduced compared to the cylindrical configuration due to the greater height of the conical configuration. This can be seen by examining the heat fluxes measured for the cylindrical test bed and comparing the corresponding power densities to the power densities measured for the conical test bed.

The cylindrical bed results are also compared to the results of the STYX experiments [4]. Description of the previous analytical work and background information of the studies can be found in [5],[6] and [7].

## 2 The test facility

The main components of the COOLOCE test facility are the pressure vessel which houses the test particle bed, the feed water and steam removal systems and instrumentation. The custom-made pressure vessel has a volume of 270 dm<sup>3</sup> and design pressure of 7 bar (overpressure). The schematic of the experimental facility is shown in Fig. 1. Fig. 2 shows a photograph of the set-up. The total volume of the conical particle bed is 17.5 dm<sup>3</sup>. The bed is 500 mm in diameter and 270 mm in height. The dimensions of the conical and cylindrical beds are illustrated in Fig. 3.

The test particle bed consists of ceramic beads that are being held in shape by a dense wire net. In the conical test set-up, lateral flooding through the surface of the cone is allowed but the geometry is not allowed to change. The particle bed is heated by resistance heating system that uses  $\varnothing$  6.3 mm vertically installed cartridge heaters. The configuration aims at achieving a uniform temperature distribution within the test bed.

In the first conical bed experiments (COOLOCE-1–2), the heaters had outer sheaths made of heat-resistant steel. Due to apparent damage to the heaters by the test conditions (high power levels, contact with steam and possible corrosion) noticed after the first experiments, modifications aiming to a more resistant configuration were made. For the cylindrical bed experiments (COOLOCE-3–5), heaters with Incoloy outer sheath were installed into the pressure vessel bottom plate that was tailored for the cylindrical bed experiments. For the new conical bed experiments (COOLOCE-6–7), the central heaters of the previous configuration were replaced with the Incoloy heaters. Separate bottom plates for the two configurations makes it possible to easily change between the geometries.

The heaters are fully covered by the porous material, there is roughly a 50 mm layer of unheated particles above the heaters. In the conical test bed, the longest heater in the centre of the test bed has a heated length of 220 mm. The length of the shortest heaters near the perimeter of the test bed is 50 mm (see [1]).

To measure the particle bed temperature and detect dryout, K type thermocouples are installed in a distributed configuration striving for maximal coverage of the particle bed volume between the heaters. The electrical connections for the heaters and thermocouples are lead through the bottom plate of the pressure vessel. The number of thermocouples in the conical set-up is 68. One of the sensors has ten measuring points, i.e. the total number of measuring points in the test bed between the heaters is 77. The number of heaters is 137, three of which are equipped with built-in temperature sensors. The location maps of the heaters and thermocouples are presented in Appendix A and Appendix B, respectively. The heating and temperature sensor configuration prior to the installation of the particle material and the complete particle bed filled with the ceramic beads are shown in Fig. 4.

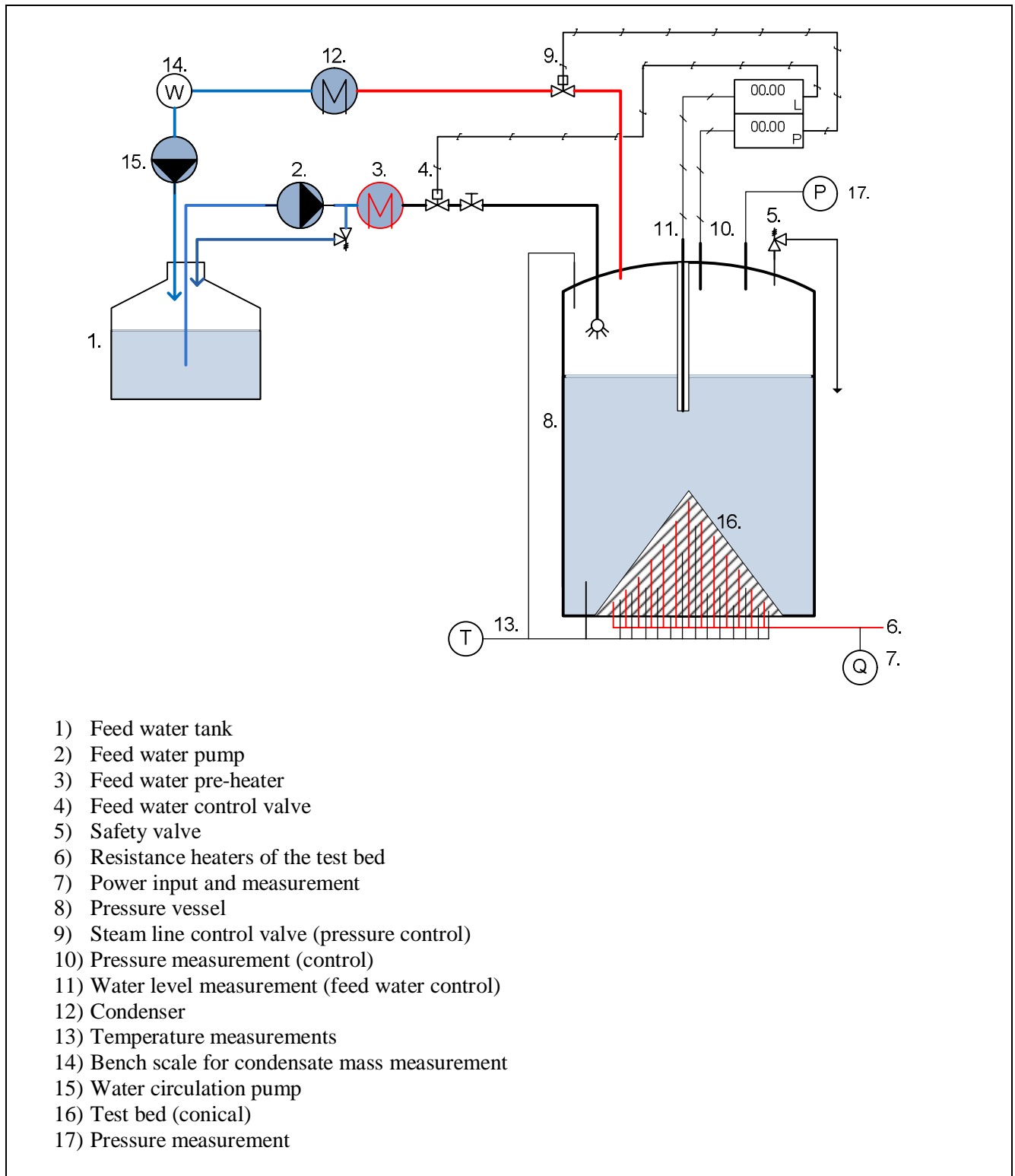
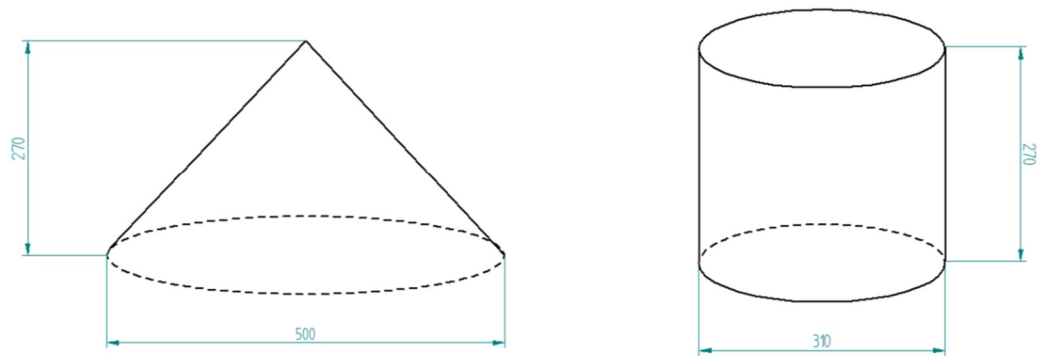


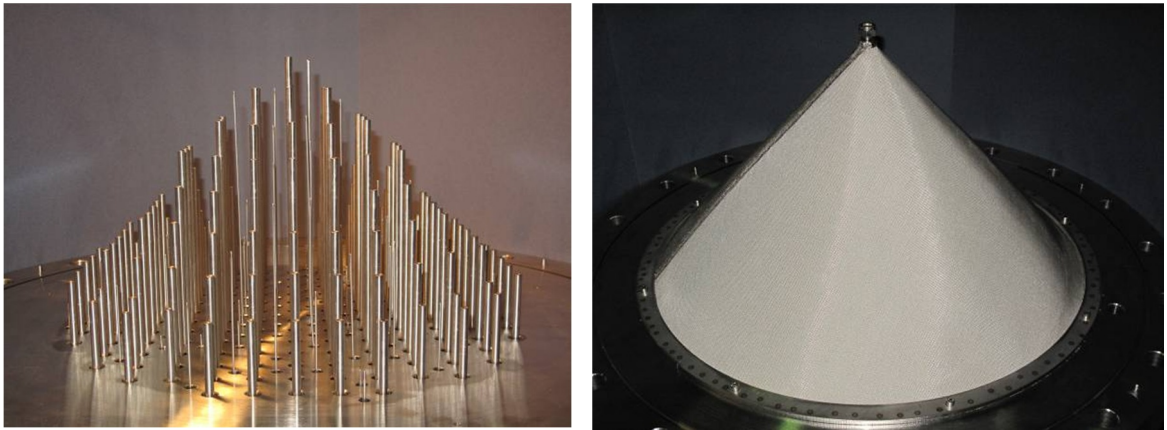
Fig. 1. The schematic flow chart of the COOLOCE test facility.



*Fig. 2. COOLOCE experimental set-up: 1) feed water pre-heater, 2) feed water control valve, 3) connection box for the heaters, 4) pressure vessel, 5) steam line condenser and scale, 6) sightglass with video monitoring, 7) water level and pressure gauges.*



*Fig. 3. Dimensions of the conical and cylindrical test beds of the COOLOCE experiments (in mm).*



*Fig. 4. The heater and thermocouple arrangement and the test bed filled with particles before the conical bed experiments. The diameter of the cone is 500 mm and the height is 270 mm.*

## 2.1 The test procedure

The test procedure consists of a heat-up sequence and the main test sequence. Generally, these are similar for the cylindrical and conical bed experiments. Prior to the experiments, the pressure vessel is filled with pre-heated water. During the heat-up sequence, heating is continued until saturation temperature and steady-state boiling has been reached. The length and power of the heat-up sequence depend on the experiment to be conducted.

In the test sequence, a stepwise power increase is conducted until a dryout is indicated by one or more thermocouples within the test particle bed. Dryout is seen as a stable increase of the sensor temperature from the saturation temperature. A holding time of 20 to 30 minutes is applied for each power step. The size of the power steps is 1 kW - 2 kW. The heating power is manually controlled by adjusting the output voltage of a purpose-tailored power transformer. The heaters are arranged in three groups according to the electrical phase. See the details in Appendix A. The water level and pressure in the test vessel are controlled by the feed water and steam line control valves according to given set points.

The test matrix for the conical bed experiments (test series 6-7) is presented in Table 1. The saturation temperature, i.e. the system temperature in the test sequence, and the evaporation energy for each test are also given.



Table 1. Test matrix for the second series of the conical bed experiments.

| Experiment | Pressure [bar abs] | Saturation temperature [°C] | Heat of evaporation [kJ/kg] |
|------------|--------------------|-----------------------------|-----------------------------|
| COOLOCE-6  | 1.1                | 102.3                       | 2250                        |
| COOLOCE-7a | 1.6                | 113.3                       | 2221                        |
| COOLOCE-7b | 2.0                | 120.2                       | 2202                        |
| COOLOCE-7c | 3.0                | 133.5                       | 2163                        |

Heat losses through the thermally insulated walls, uninsulated bottom plate and connections of the test vessel cause the power consumed by boiling to be smaller than the control power. Also, since the capacity of the feed water pre-heater is not high enough to increase the feed water temperature to boiling point, maintaining the saturation temperature has to be done by the heaters. The pre-heater increases the feed water temperature up to about 60-90°C.

Because of this, the boiling rate is verified by measurements of the condensing steam mass flow rate. The measurement is done by directing the condensate flow to a bench scale with online measurement of mass. The condensate container is emptied sequentially after the mass flow reading has been obtained. The water is then re-circulated back into the feed water tank.

The power calculated from the condensate mass during the time step that leads to dryout gives an estimate of the actual dryout power and the heat losses of the system. This *calculated power* includes uncertainties such as the effect of possible direct contact condensation within the test vessel. Nevertheless, we consider the calculated value to be more accurate than the *control power* (the electrical output power) especially at lower pressure levels. At higher pressure levels, the role of condensation in the test vessel and on the test vessel walls may be greater, causing the steam flow to the condenser to fluctuate. This is due to the lower temperature and greater mass flow rate of the feed water, as well as the greater temperature difference to the environment.

### 3 Experimental results

In the conical particle bed experiments (test series 6 and 7) four dryout points were measured within the pressure range of 1 to 3 bars.

#### 3.1 COOLOCE-6

The first experiment with the re-installed conical debris bed COOLOCE-6 was conducted at nominally atmospheric pressure. For this, the control valve of the steam line was removed to verify that the pressure remained nearly atmospheric. (Otherwise, the pressure could increase due to flow resistance of the valve, even if it was fully open, as seen in COOLOCE-2.)

Dryout was observed at the control power of 26.0 kW using 2 kW power steps. During the first “approach” towards dryout, 5 kW power steps were applied. When dryout was seen at approximately 25 kW, the power was switched off and a new approach with the smaller 2 kW power steps was made. The power and temperature history of the experiment are shown in Fig. 5.

A detail of the temperature and power history near dryout is shown in Fig. 6. It is seen that the temperature of the sensor 117-135 at 17 cm from the bottom of the bed increased close to 200°C before the experiment was terminated. The sensors 115-135, 114-315 and 117-45 at the heights of 15 cm, 14 cm and 17 cm near the centre of the test bed (zone 1 in Appendix B) followed with a more modest temperature increase. At the power level of 20 kW and above, two heater sensors, T69 and T70, showed temperatures somewhat above the saturation temperature. A further increase was seen during the last two power steps, the latter of which was the dryout power step indicated by the sensors in the test bed between the heaters (in the porous material).

It should be noticed that in this experiment and in all the following experiments, the reported control power is based on manually recorded values from the power analyser. This is because of a suspected malfunction in the output module of the power analyser, causing the power value recorded online to deviate from the input values by 1-2 kW.

The pressure and water level in the test vessel as well as the feed water temperature during the test are shown in Fig. 7. At the control power level leading to dryout (26.0 kW), the approximate mass flow rate based on the water collected on the scale was 0.0105 kg/s. The power corresponding to this steam production rate is 23.7 kW.

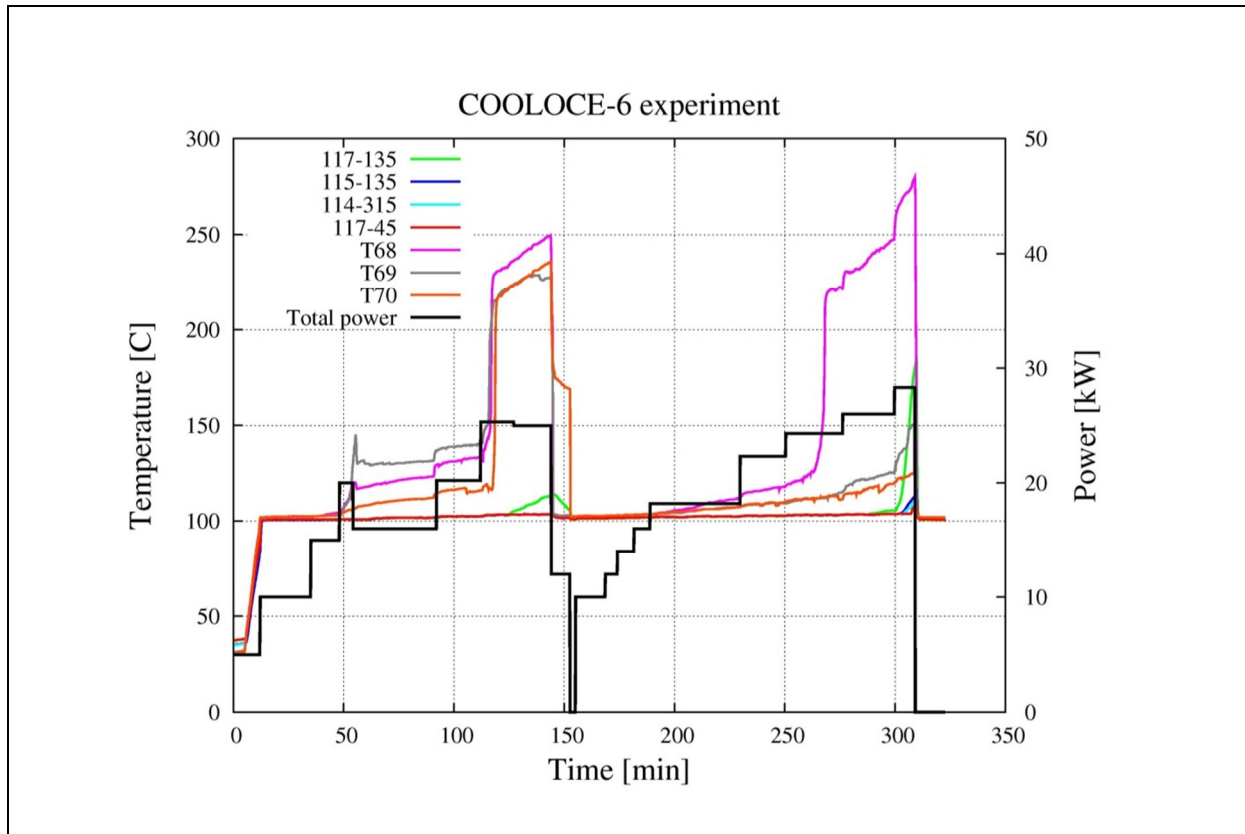


Fig. 5. Control power and temperature log in the COOLOCE-6 experiment at the pressure of 1.1 bar (not pressurized). T68-70 indicate the heater sensors.

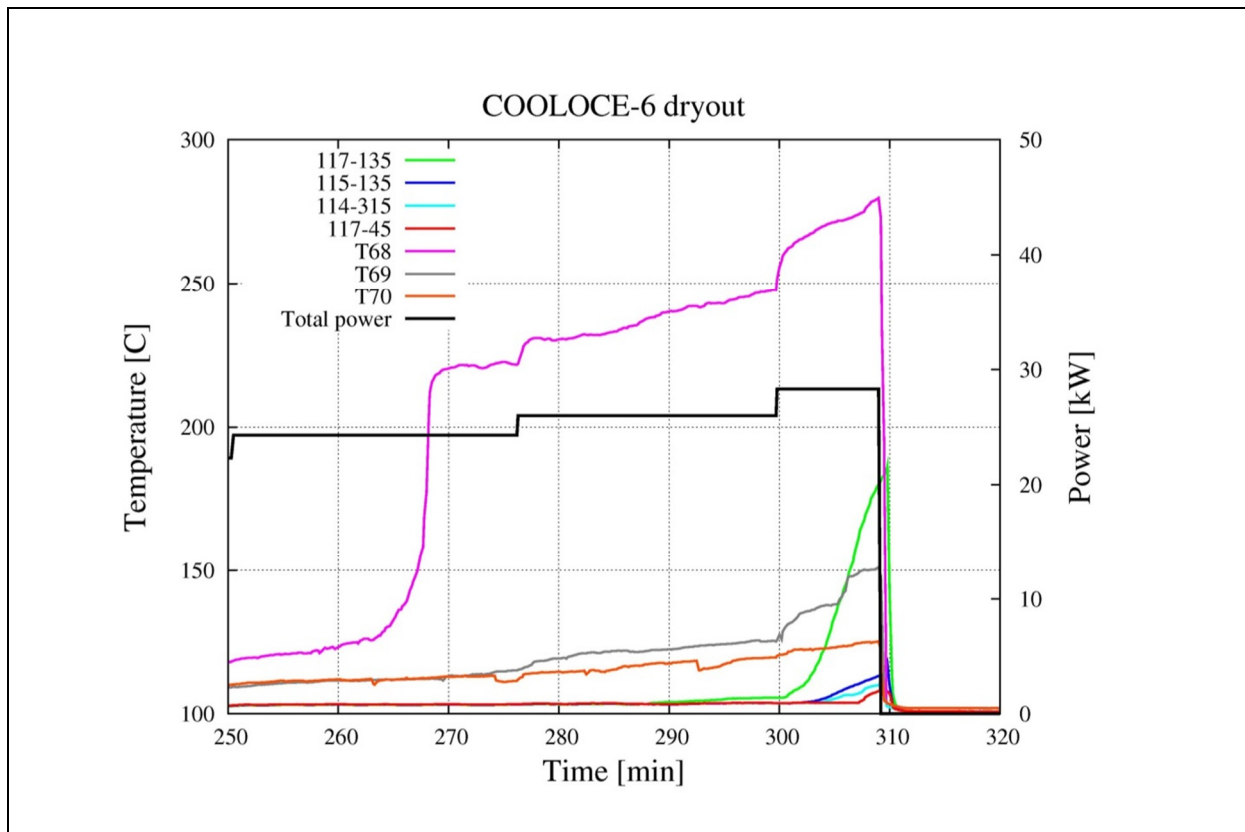


Fig. 6. Control power and temperature in the COOLOCE-6 experiment during the final power steps and dryout.

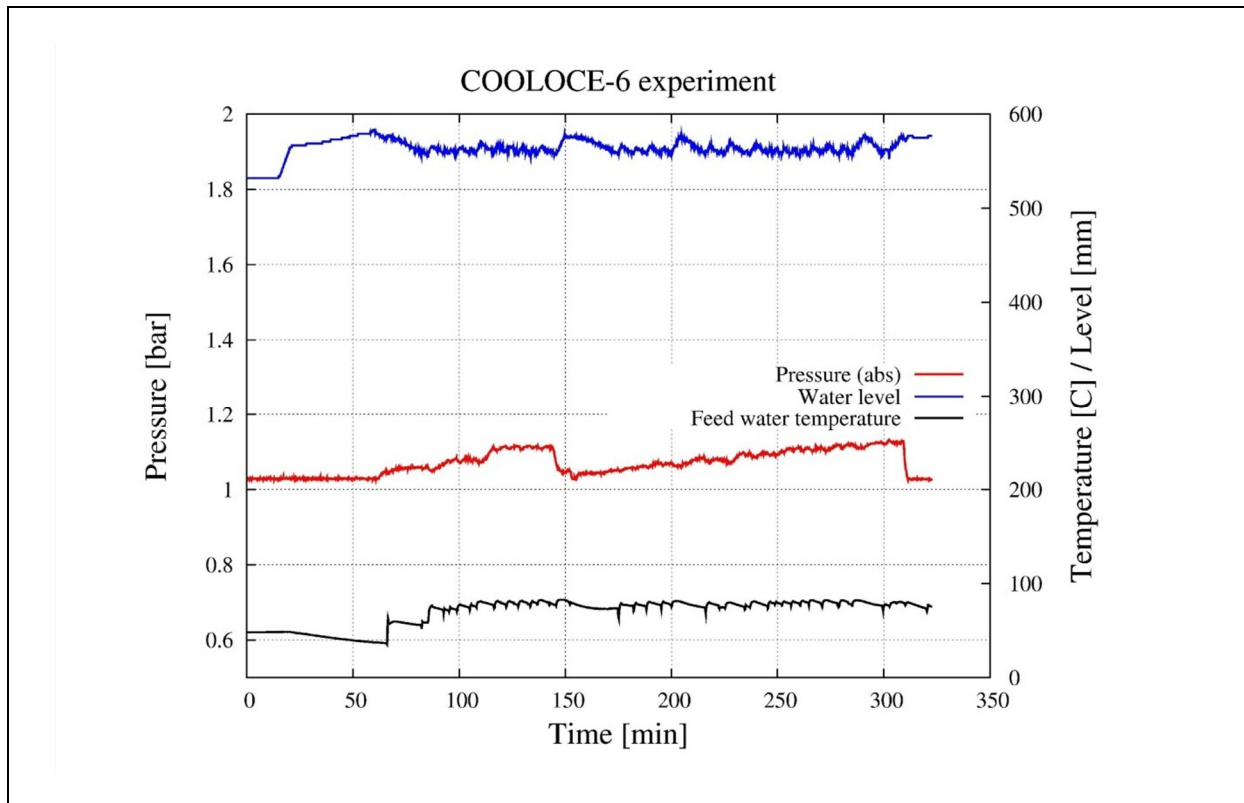


Fig. 7. Pressure and water level in the test vessel and the feed water temperature during the COOLOCE-6 experiment.

### 3.2 COOLOCE-7a, -7b and -7c

The COOLOCE-7 test run consisted of the pressure levels of 1.6 bar (a), 2.0 bar (b) and 3.0 bar (c). In the 1.6 bar experiment, dryout at the control power of 31.8 kW was seen. Dryout was indicated by the temperature sensor 117-135. Spreading of dryout to the sensors 117-45, 115-135, 114-315 and 118-225 was seen after a further power increase up to 34.1 kW. This means that all the innermost (zone 1) sensors between the heights of 140 mm and 180 mm reached dryout after a 2 kW increase from the incipient dryout. The most pronounced temperature increase was at the sensor 117-135 which reached 240°C before power was switched off. Also, the heater sensors showed a modest increase from saturation temperature.

The temperatures of the test bed sensors indicating dryout and the heater sensors and the power history of the COOLOCE-7a experiment are shown in Fig. 8. A detail of the power and temperature during the final power steps is shown in Fig. 9. The water level and pressure and the feed water temperature are shown in Fig. 10. At the dryout power level, the condensate mass flow was approximately 0.0133 kg/s which corresponds to a power of 29.6 kW.

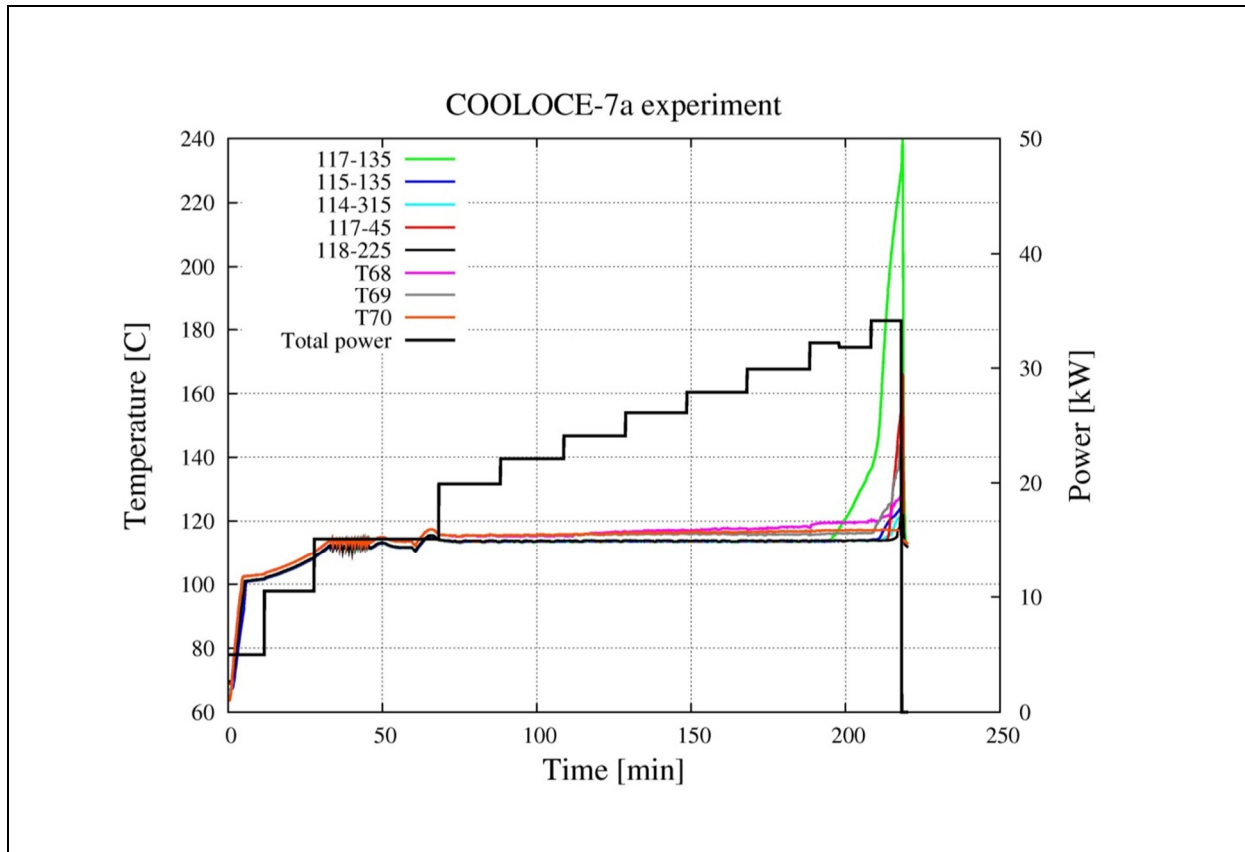


Fig. 8. Control power and temperature log in the COOLOCE-7a experiment at the pressure of 1.6 bar. T68-70 indicate the heater sensors.

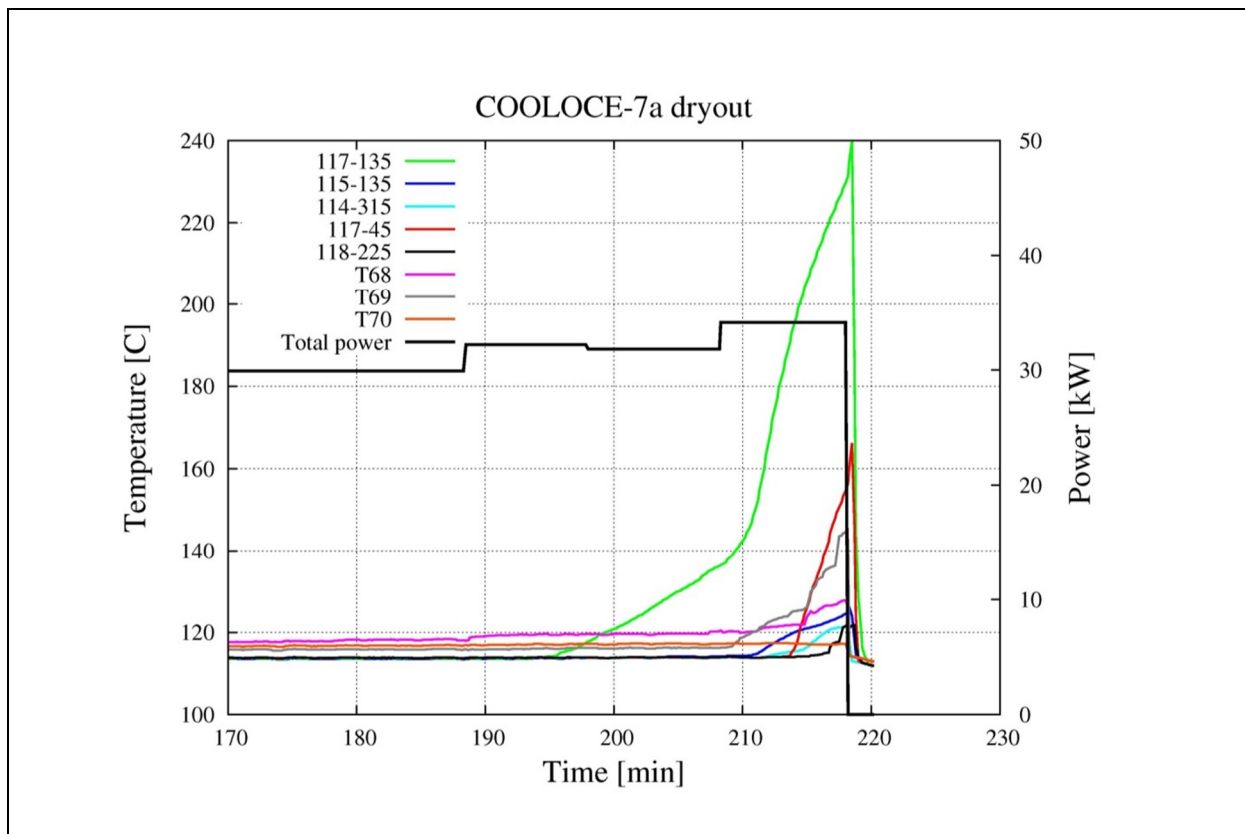


Fig. 9. Control power and temperature during the final power steps and dryout in the COOLOCE-7a experiment.

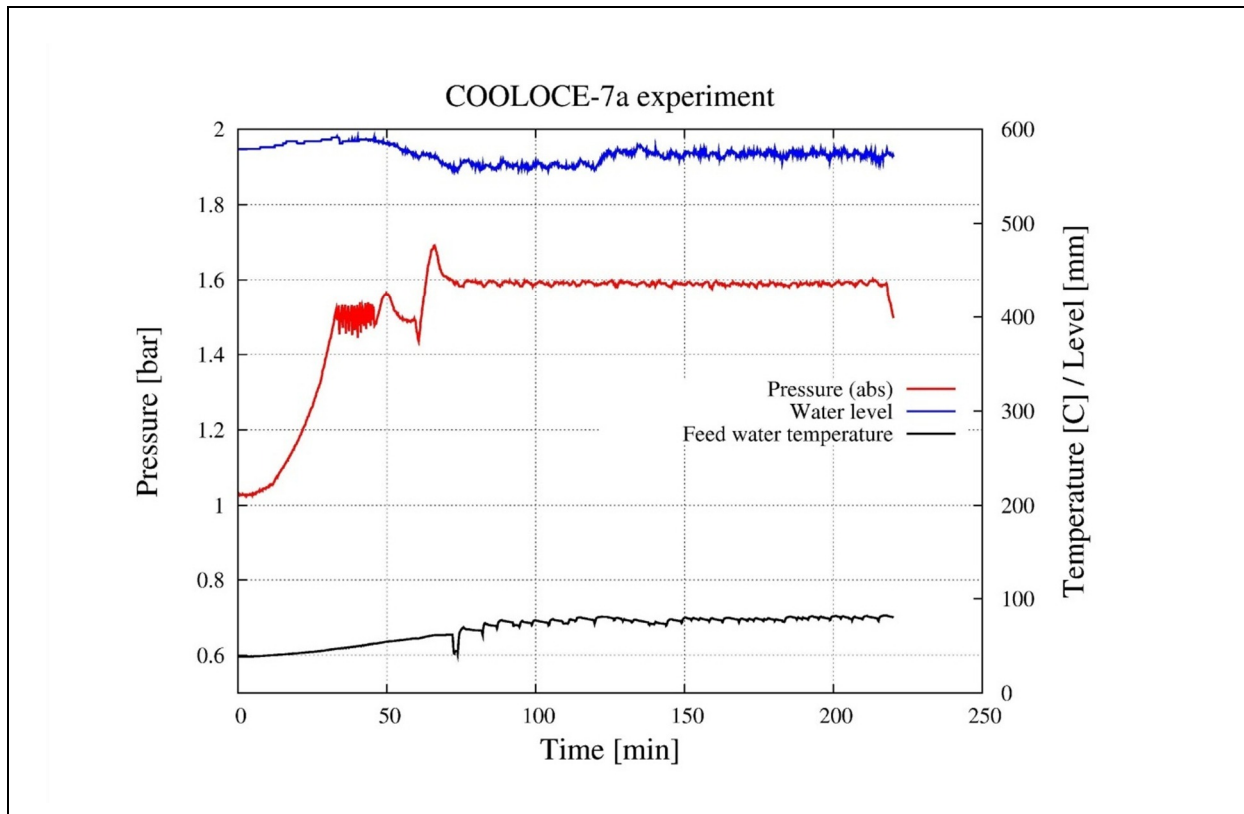


Fig. 10. Water level and pressure in the test vessel and the feed water temperature in the COOLOCE-7a experiment.

In the 2.0 bar experiment, dryout was seen at the control power of 36.0 kW, indicated by the central multi-point sensor at 170 mm from the test bed bottom. Dryout spread to the sensors points 120-135 and 115-135 of the multi-point sensor but not before control power was further increased to 38.3 kW. The power was switched off when the sensor 117-135 had reached 190°C. Only a slight increase was observed in the heater sensors apparently due to the location of the built-in sensor which is at the height 100 mm, and thus lower than the location of dryout. The surface temperature higher in the heating rods is not known.

The temperatures of the test bed sensors indicating dryout and the heater sensors and the power history of the COOLOCE-7b experiment are shown in Fig. 11. A close-up of the dryout phase is shown in Fig. 12. The water level and pressure and the feed water temperature are shown in Fig. 13. Based on the condensate mass flow of about 0.0144 kg/s, the heat flow directed to boiling was 31.6 kW.

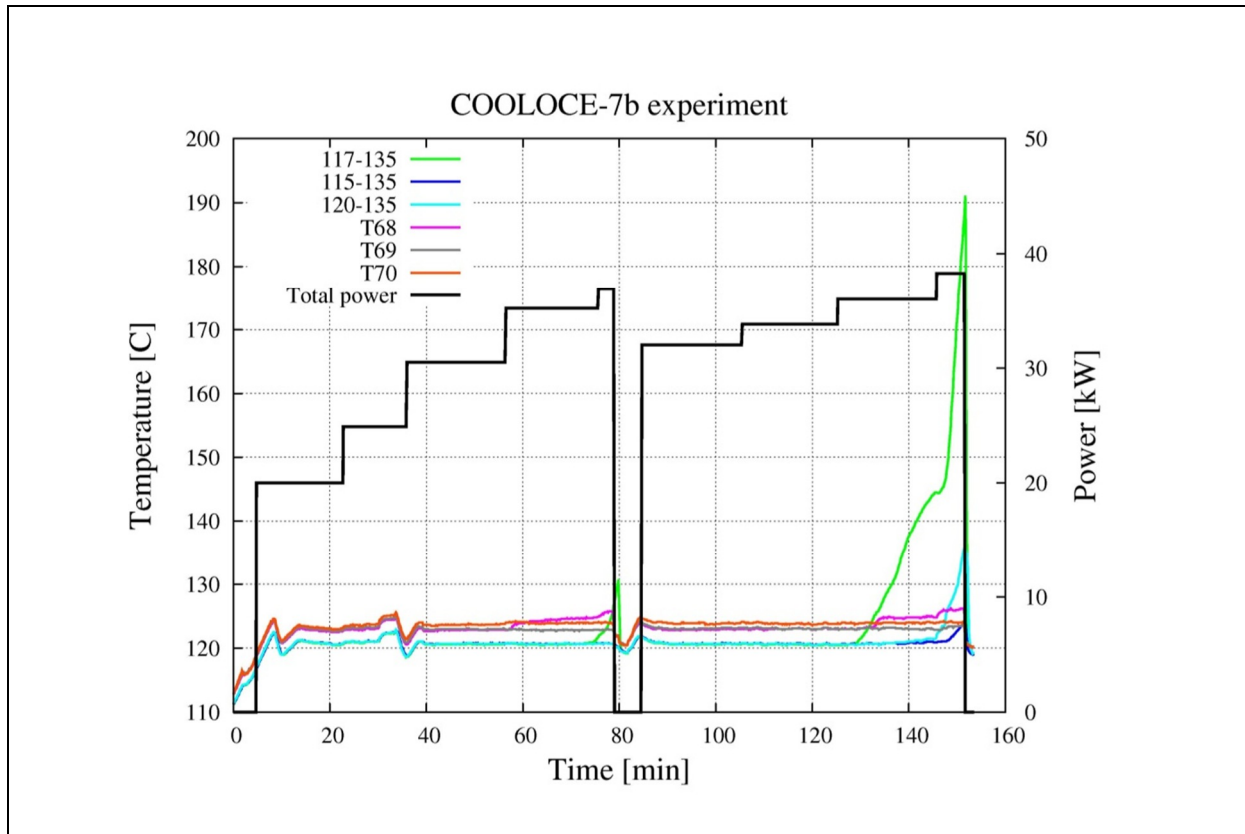


Fig. 11. Control power and temperature log in the COOLOCE-7b experiment at the pressure of 2.0 bar. T68-70 indicate the heater sensors.

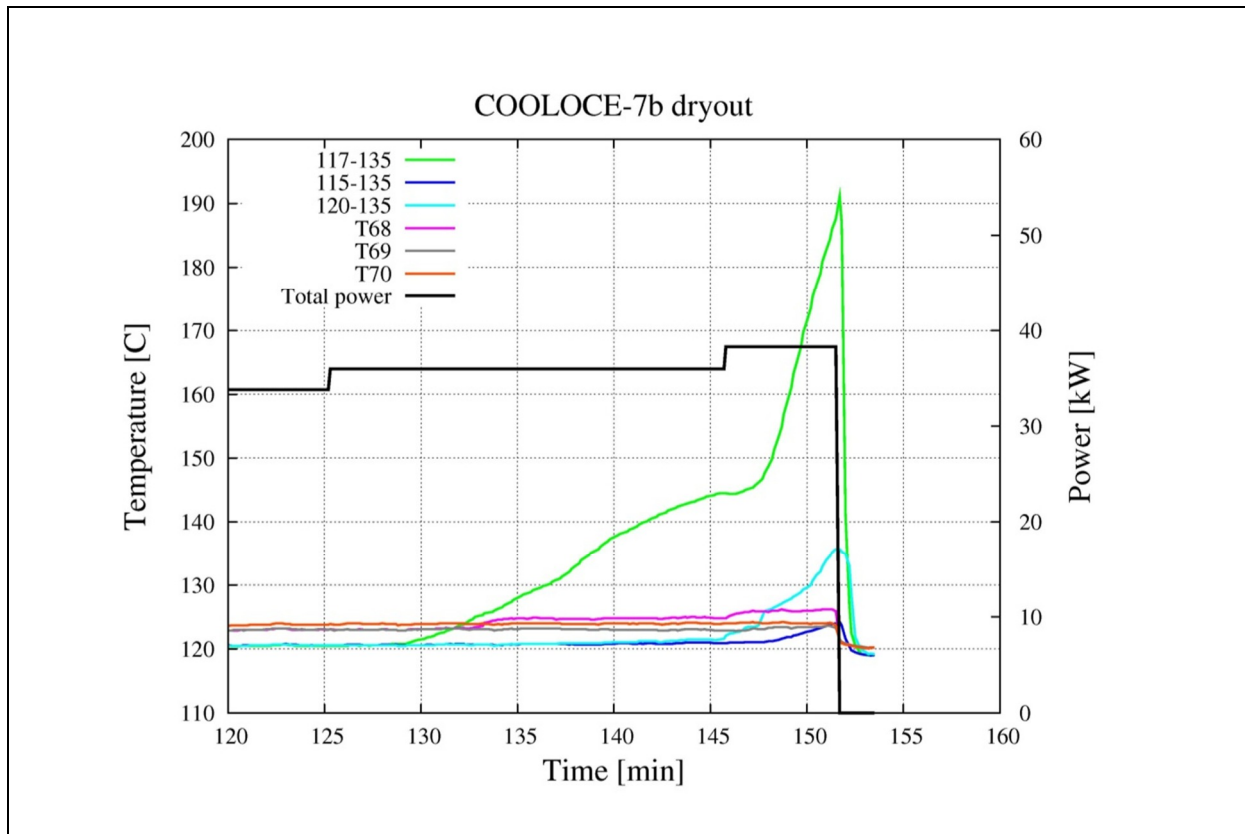


Fig. 12. Control power and temperature during the final power steps and dryout in the COOLOCE-7b experiment.

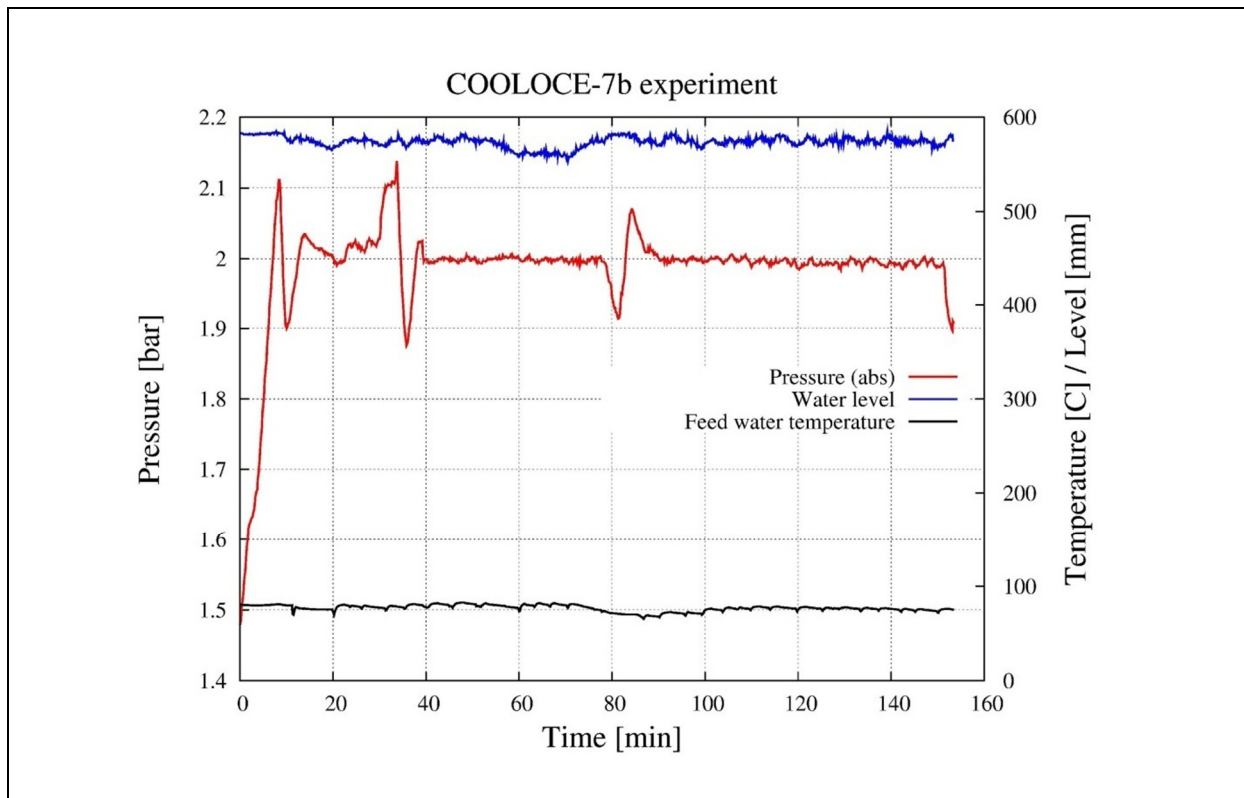


Fig. 13. Water level and pressure in the test vessel and the feed water temperature in the COOLOCE-7b experiment.

In the 3.0 bar experiment, the sensor 117-135 (same as in the previous experiment) indicated dryout at the control power of 42.9 kW. A very small deviation from saturation temperature is seen in the sensor 120-135. The temperatures of the sensors indicating dryout and the heater sensors as well as the power history of the COOLOCE-7c experiment are shown in Fig. 14.

The power was switched off when it was noticed that the power of the heaters connected to the central phase started to show fluctuations. A drop in the temperature of the central heater occurred around the same time (T69 at 120 minutes into the test sequence). This was interpreted as possible heater damage and the test sequence was terminated. However, after a brief inspection of the heaters and the safety fuses, the test was continued. A second dryout followed but at a higher power level of 45.6 kW. Because of the suspected heater damage, the test sequence was stopped after the second dryout, preventing experiments at higher pressures.

The first measured dryout is taken to be the result of the experiment because of the suspected heater damage which may distort the results. The central heaters are crucial in the heating configuration because dryout is expected to be formed into the central upper part of the geometry. The loss of heating power in the central heating rod would cause a cooler spot – or a type of channel – into the test bed in which case dryout would be transferred to outer and lower (heated) parts of the cone. This is also expected to increase the power needed for dryout.



A close-up of the power and temperature histories during the power steps leading to dryout is presented in Fig. 15. The water level and pressure and the feed water temperature in the COOLOCE-7c experiment are shown in Fig. 16. At the dryout power level, the average mass flow rate of condensate was approximately 0.0166 kg/s which corresponds to a heat flow of 35.9 kW.

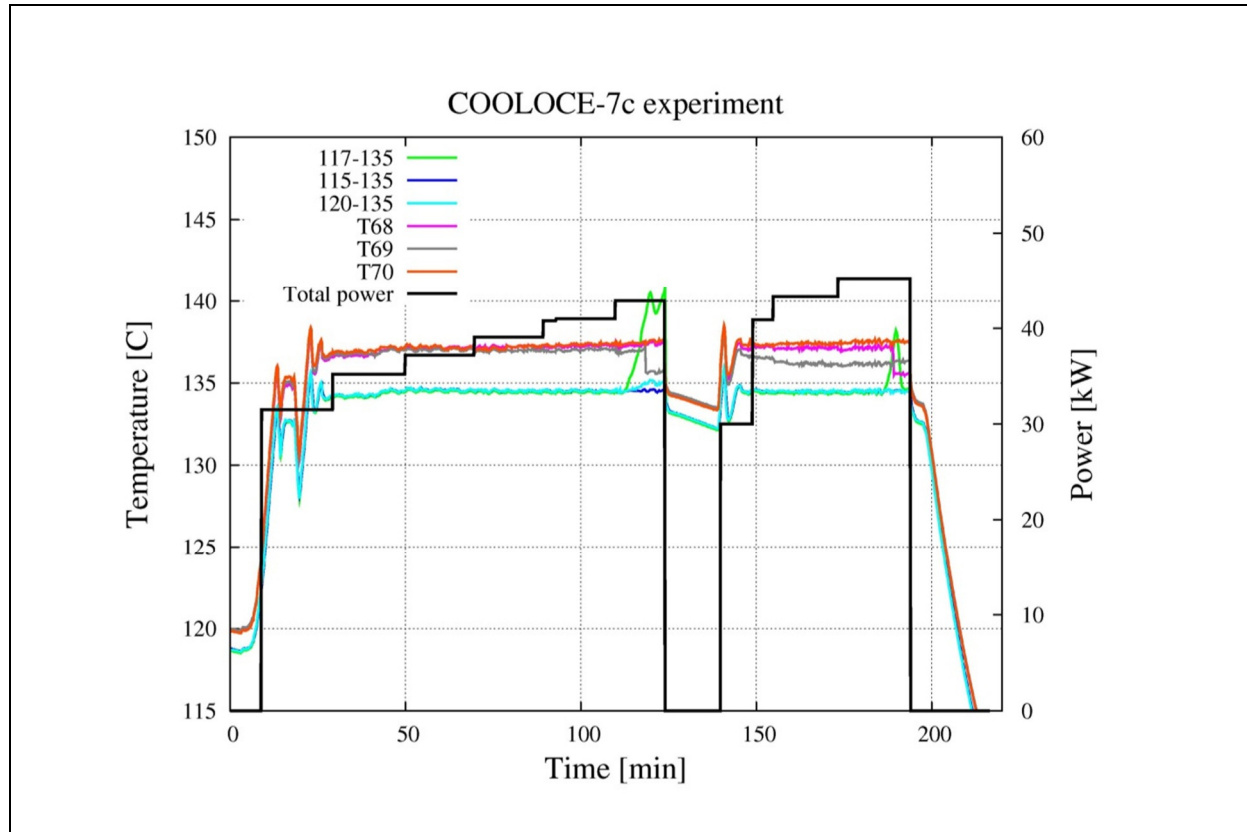


Fig. 14. Control power and temperature log in the COOLOCE-7c experiment at the pressure of 3.0 bar. T68-70 indicate the heater sensors.

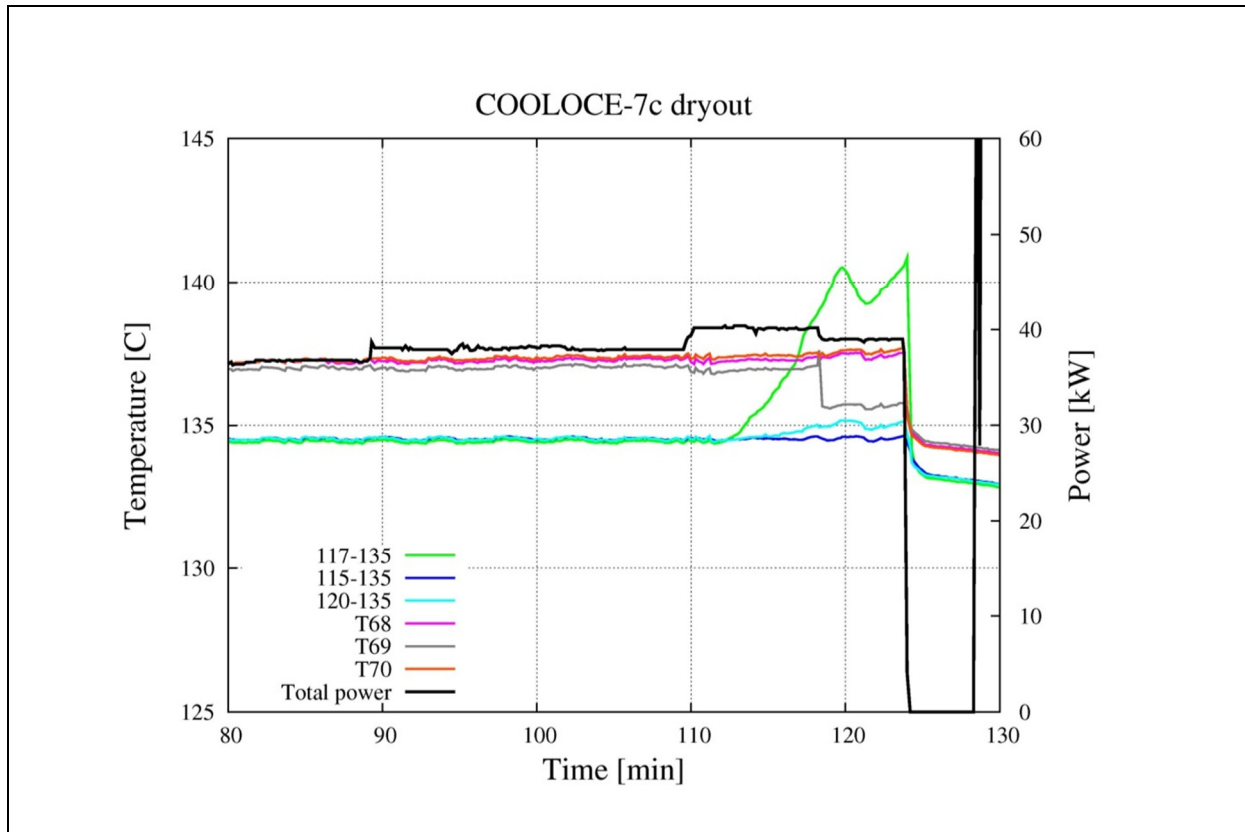


Fig. 15. Control power and temperature during the final power steps and dryout in the COOLOCE-7c experiment.

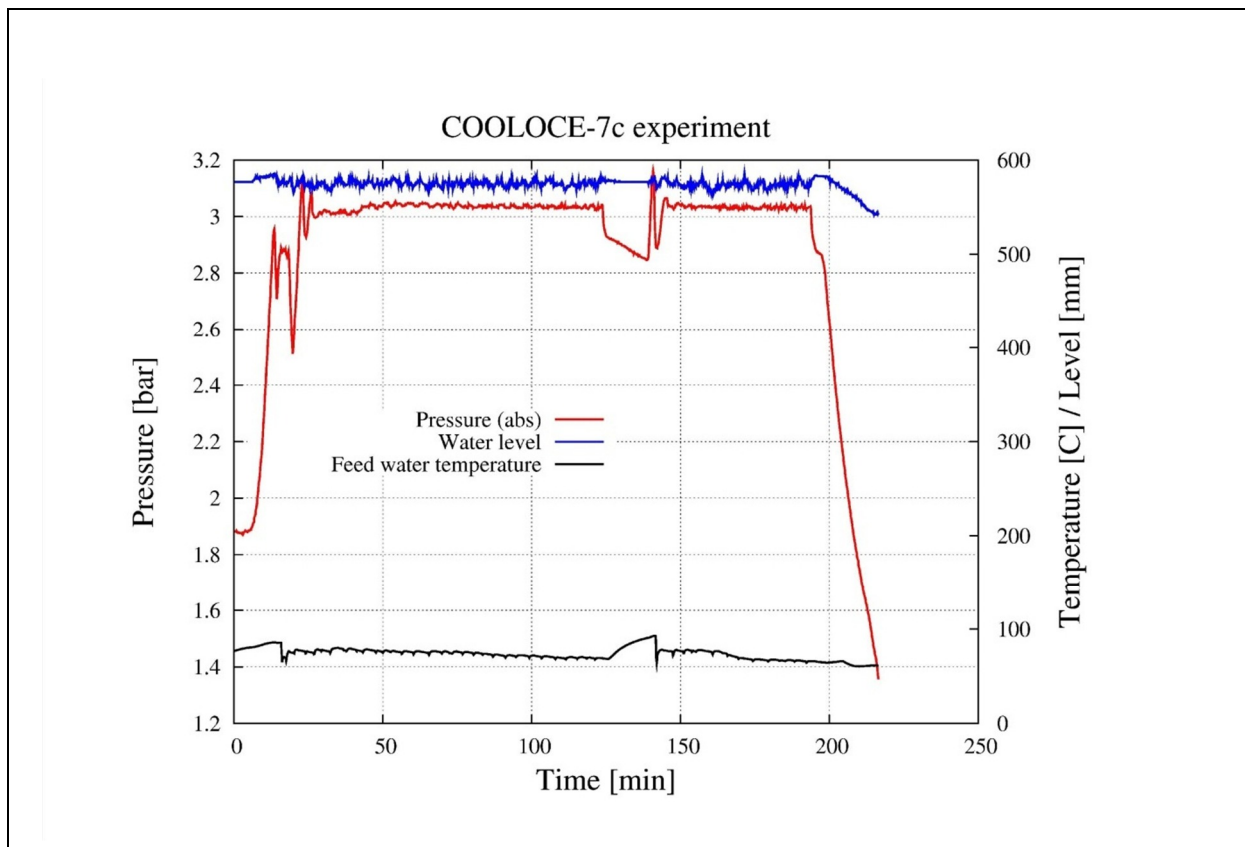


Fig. 16. Water level and pressure in the test vessel and the feed water temperature in the COOLOCE-7c experiment.

## 4 Analysis

In this Chapter, a general analysis of the test results is presented as well as the comparison of the dryout behaviour of the cylindrical and conical debris beds based on the results of the COOLOCE test series 1 – 7. A comparison of the cylindrical bed results to the STYX experiments is also given.

The most important comparison is the one between the two geometries. In power plant scenarios, the formation of a heap-like particle bed is possible as a result of gradual melt release after the failure of the reactor pressure vessel. However, traditional analyses have focused on top-flooded particle bed configurations, without taking into account realistic geometries. From the safety point of view, it is of high importance to extend the investigations to prototypic scenarios and verify the coolability of conical or heap-like geometries. Further analysis and in-depth consideration of the application of the experimental results to reactor scenarios will be presented later with the numerical analysis of the experiments.

### 4.1 Control power and calculated power

In the COOLOCE experiments, the heating power directed to boiling was estimated based on the mass of condensate measured by a scale connected to the outlet of the heat exchanger. The calculated power  $P_{calc}$  is the condensate mass flow rate  $q_m$  (kg/s) multiplied by the latent heat of evaporation  $h_{fg}$ , (kJ/kg) during the power step that leads to dryout:

$$P_{calc} = q_m \cdot h_{fg} \quad (1)$$

The calculation assumes that the water which is collected at the outlet is equal to the mass that has been evaporated by the heated test bed. The comparisons of the control power and the calculated power are presented in Fig. 17 for the conical test bed and in Fig. 18 for the cylindrical test bed.

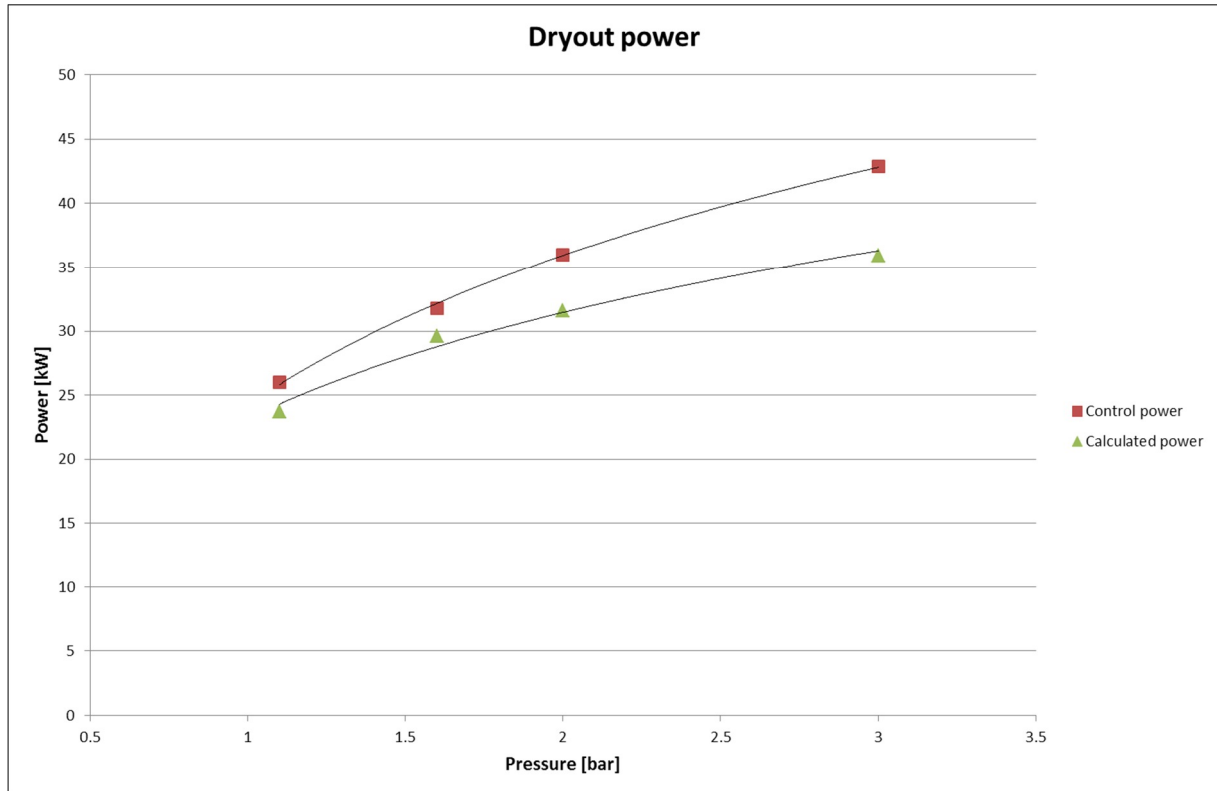


Fig. 17. Control power and calculated power in the conical bed experiments.

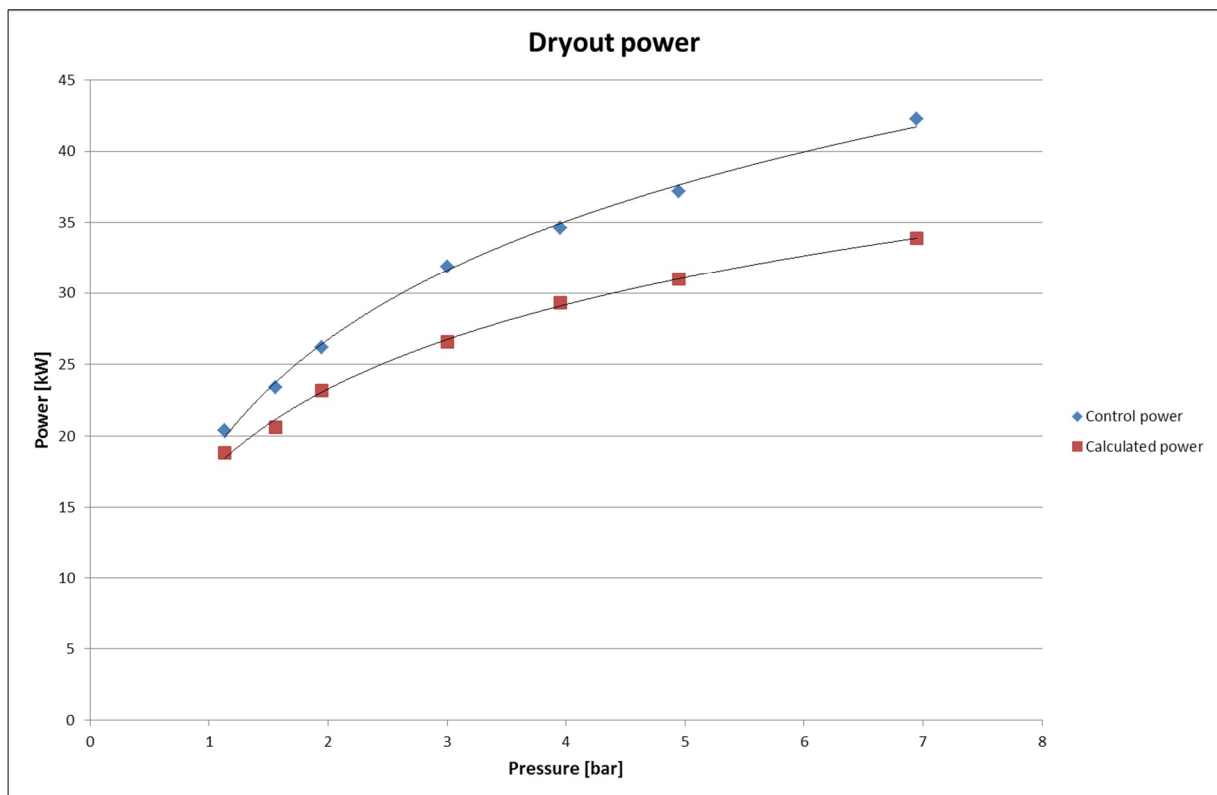


Fig. 18. Control power and calculated power in the cylindrical bed experiments.

It is seen that the control power differs from the calculated power by roughly 2 – 8 kW (7 – 20%). The heat losses to the environment contribute to the difference. It

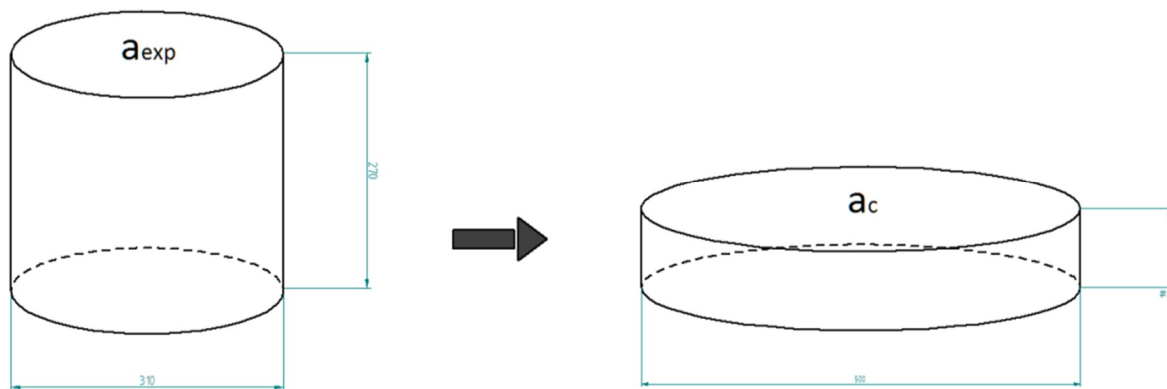
is also seen that the relative difference between the power values increases as a function of pressure. The calculated power is smaller for higher pressures. The calculated power might be too low at pressure levels above 2 bar because the higher the pressure, the greater is the difference between the feed water temperature and the saturation temperature. This leads to that 1) more power is consumed by maintaining the saturation temperature and 2) steam condensation in the test vessel is increased, reducing the flow to the condenser.

The effect of direct contact condensation, i.e. the condensation of steam back to liquid before it reaches the steam line can not be estimated with the available data. Nevertheless, the verification of the boiling power by the mass flow measurement gives valuable information for reducing the uncertainties of the test set-up. In the next section, for the sake of clarity we use the value of control power for comparison between the conical and cylindrical geometries.

## 4.2 Comparison of the conical and cylindrical bed results

Dryout power for four pressure levels (1.1 bar, 1.6 bar, 2.0 bar and 3.0 bar) have been measured for both conical and cylindrical test beds. Based on these measurements, evaluation of effect of the particle bed geometry can be made. The conical and cylindrical debris beds of the COOLOCE test facility have similar height and roughly the same volume. However, for reactor scenarios concerning ex-vessel debris formation, it is more interesting to compare two beds that have a similar diameter and volume because the spreading of the debris is limited by the walls of the containment drywell. Debris that is evenly distributed in the spreading area forms a cylindrical configuration with coolant infiltration through the top surface.

The results of the cylindrical bed experiments may be translated to represent a low bed with the same volume and diameter as the conical bed by a simple scaling procedure. The scaling is illustrated in Fig. 19.



*Fig. 19. The scaling of the cylinder of the COOLOCE experiments to a comparison cylinder that has the same diameter as the COOLOCE cone. The diameter of the comparison cylinder is 500 mm and the height is 90 mm.*

The coolability of a symmetric top-flooded bed is determined by its dryout heat flux ( $\text{kW/m}^2$ ) which is independent of the bed height for deep beds. The total dryout power that corresponds to the measured dryout heat flux in a bed of different dimensions may be calculated using the bed surface area. The heat flux for the experimental cylinder  $q''_{exp}$  is defined as

$$q''_{exp} = \frac{P_{exp}}{a_{exp}} \quad (2)$$

where  $P_{exp}$  is the experimental total power and  $a_{exp}$  is the area of the experimental cylinder. The total power  $P_c$  for a cylinder whose area is  $a_c$  is

$$P_c = q''_{exp} * a_c \quad (3)$$

We call this cylinder with the experimental heat flux and a calculated total power the *comparison cylinder*. The comparison cylinder has a new power density  $q'''_{exp}$  ( $\text{kW/m}^3$ ) which is the total power divided by the bed volume  $V_{exp}$  or the heat flux divided by the height  $h_c$  of the comparison cylinder

$$q'''_{exp} = \frac{P_c}{V_{exp}} = \frac{q''_{exp}}{h_c} \quad (4)$$

Note that the calculation of a new dryout power presumes that no other parameter of the bed (aside from its dimensions) is changed in the scaling.

Fig. 20 summarizes the results for (1) the experimental conical bed, (2) the experimental cylindrical bed and (3) the comparison cylinder. Because the experimental cylinder and cone have slightly different volumes, the comparison is given as power densities (total power divided by the particle bed total volume).

It is seen that the dryout power density for the experimental conical bed is 49 – 60% greater than for the experimental cylinder. This is due to the multi-dimensional water infiltration and co-current flow of water and steam within the conical bed which improve coolability compared to infiltration through the top surface.

However, the power densities for the experimental cone are smaller than for the comparison cylinder by 47 – 51%. In this case, the cylindrical bed surface area is so large that for a constant heat flux  $q''$ , the total power needed for dryout becomes larger than the corresponding power for the conical bed. In other words, the experiments suggest that the coolability of a conical configuration is approximately 50% poorer than that of a cylindrical configuration if the two configurations have equal diameter and volume.

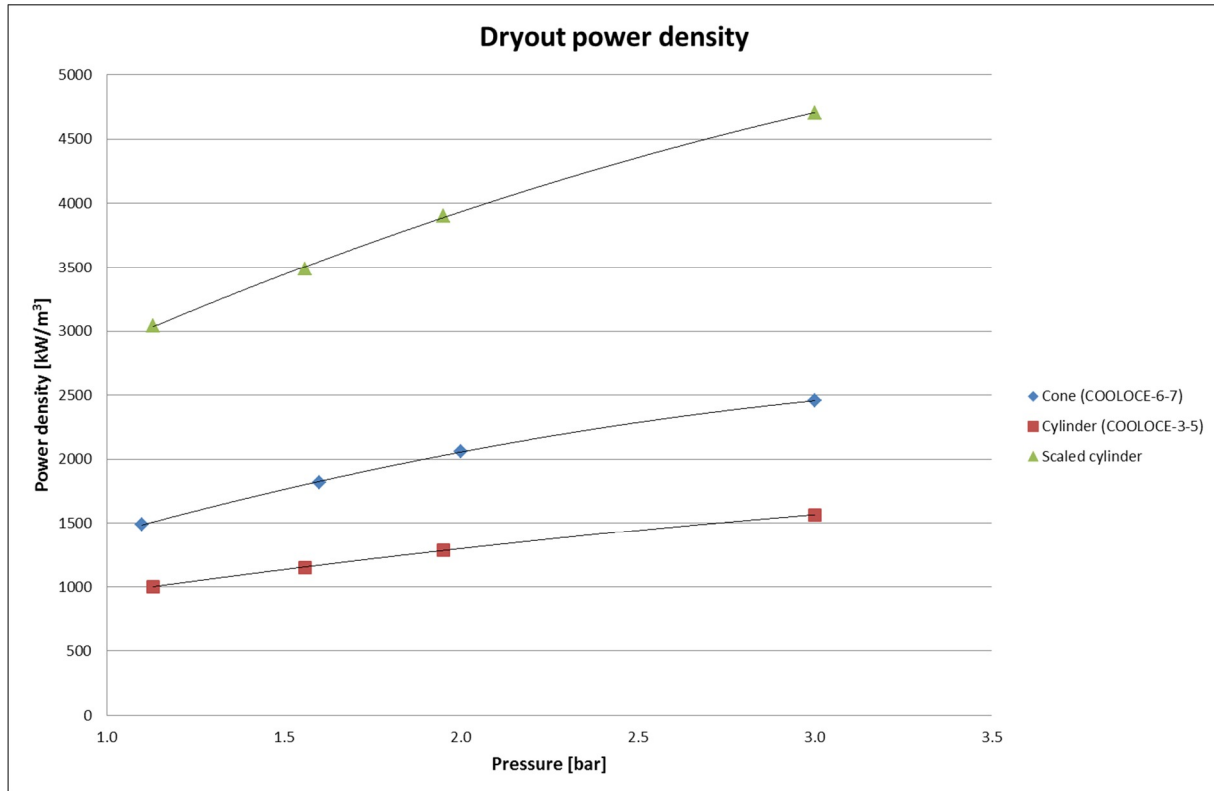


Fig. 20. The comparison of dryout power densities measured for the COOLOCE cone and cylinder and the comparison cylinder used in analyzing the effect of geometry.

For example, in the COOLOCE-3R experiment, the dryout power was 20.4 kW. The surface area of the experimental cylinder is  $0.0755 \text{ m}^2$ . The surface area of the comparison cylinder is  $0.196 \text{ m}^2$ . For the dryout heat flux (Eq. 2), this yields  $270.2 \text{ kW/m}^2$ . Then, the value of the comparison power is 53.0 kW according to Eq. 3. The corresponding power density is  $3029 \text{ kW/m}^3$ .

It is well known that the presence of multi-dimensional water infiltration increases dryout power, and helps to maintain the conical configuration in a coolable state. On the other hand, due to the greater height of the conical configuration, steam has to travel a longer distance to escape the debris bed. The conical debris bed is three times higher than the flat-shaped, cylindrical debris bed (as seen directly from the geometry of the three-dimensional objects).

In a homogeneously heated conical bed, heat flux increases proportionally to the increase of the height of the examined cross-section. In general, this is true also for cylindrical beds and other homogeneously heated geometries. The problem with the conical bed is that the heat flux in the upper parts of the cone is greater compared to the corresponding heat flux – or mass flux density of steam – at the top surface of a flat-shaped cylinder. The present experimental results suggest that the effect of the increased height of the debris bed which decreases coolability is more significant than the effect of the multi-dimensional flooding which increases coolability. Thus, a top-flooded cylinder can not be considered to be the most conservative debris bed geometry.

Concerning the coolability in plant-scale assessment, the following limitations of the above analysis should be noticed:

- 1) The post-dryout behaviour of the conical debris bed is expected to differ from that of the cylindrical bed. The conical bed might reach post-dryout steady-states in which the steam flow plays a role in maintaining coolability. However, this is beyond the scope of the present study in which we consider the formation of the incipient dryout to be the limit of coolability.
- 2) Dryout in the upper and central parts of the conical geometry was clearly seen in the experiments. On the other hand, numerical simulations suggest that dryout in the conical configuration occurs in a small region near the tip of the cone where the critical heat flux is first exceeded [1], [2]. The formation of such a small incipient dryout might be impossible to detect in experimental conditions. We recommend that the latest knowledge of the realistic shape and possible deformation of the debris bed is taken into account in future studies. This would be especially important for code validation.

### 4.3 Comparison to the STYX experiments

Another interesting comparison is how the present results relate to the results of the STYX experiments with a 600 mm high homogenous test bed. In the COOLOCE cylindrical bed experiments as well as the STYX experiments the pressure range was 1 – 7 bar. Irregular alumina particles were used in the STYX experiments. The effective diameter of the particles based on pressure drop measurements and the Ergun's equation for porous media was 0.8 mm [7]. The spherical particles of the COOLOCE experiments have a diameter of 0.8 mm – 1.0 mm.

The porosity of the STYX test beds was evaluated to be 0.34 – 0.4 with 0.37 as the most commonly used value in analyses. The porosity of the COOLOCE test beds was estimated by filling the dry bed with water. This yielded a porosity of about 0.38. The porosity according to the maximum random packing density of spherical particles is 0.36 - 0.37 which indicates that the measured result is reasonable.

The important bed parameters are reasonably close to each other in the COOLOCE and STYX experiments so that a comparison can be made. The dryout heat fluxes (dryout power divided by the bed surface area) for the COOLOCE experiments and STYX-8 experiments as a function of pressure are plotted in Fig. 21. For the COOLOCE experiments, value based on both the control power and calculated power are given.



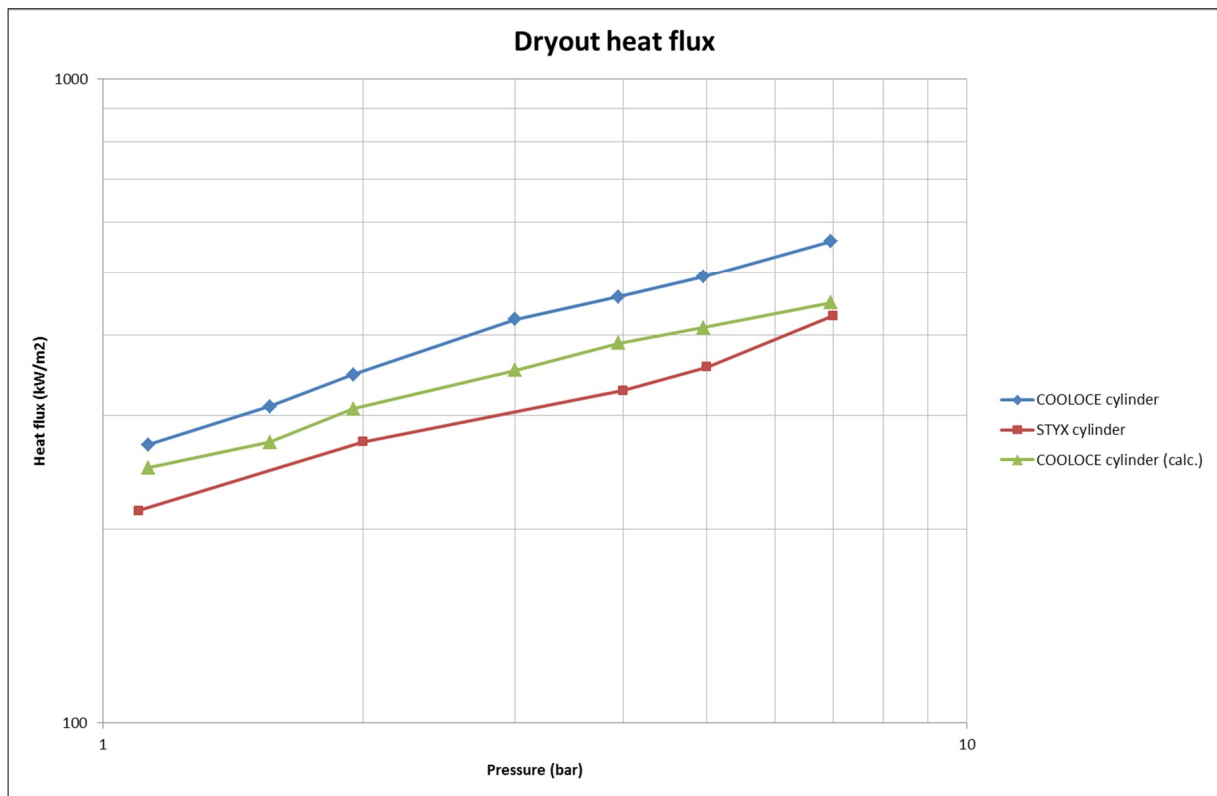


Fig. 21. Comparison of the dryout heat fluxes of the COOLOCE cylindrical bed experiments and the STYX cylindrical bed experiments.

The measured heat fluxes for the COOLOCE test bed are 27 – 40% greater than for the STYX test bed for the control power and 5 – 18% for the calculated power. It is possible that this is due to a downcomer effect caused by the vertical heating arrangement in the COOLOCE facility and the slightly different particle size. In the STYX test bed, the heating arrangement consisted of heating wires located at different horizontal levels. It can be expected that the flow patterns within the test medium for these two heating methods are different.

It should be kept in mind that the comparison addresses two different test set-ups which differ from each other in the following:

- 1) The heating arrangement (power distribution)
- 2) The location and density of the thermocouples used to detect dryout
- 3) The particle material
- 4) The thermal insulations

A more accurate estimation of the effect of the heating arrangement and reduction of the uncertainties related to the two test set-ups could be obtained by experiments using the alumina gravel of the STYX tests with the COOLOCE test facility. The new results could then be compared to the existing cylindrical bed experiments.

## 5 Discussion and summary

The experiments conducted within the COOLOCE test programme are summarized in Table 2. The COOLOCE-0 test was a preliminary experiment conducted in order to verify that heaters and instrumentation were working as required. The maximum control power applied in the preliminary experiment was 20 kW (for which no dryout was seen). The COOLOCE-1 – 2 test series were performed with the conical particle bed and the COOLOCE-3 – 5 series with the cylindrical bed. After the cylindrical bed test series, improvements were made to the conical bed and a new series with the conical test bed was conducted (COOLOCE-6 – 7).

*Table 2. Summary of the COOLOCE experiments in chronological order. Dryout power density and heat flux are given for the control power. Heat flux is given only for the cylindrical bed because a directly comparable heat flux does not exist for the conical bed.*

| Experiment                   | Date          | Pressure [bar] | Dryout results     |                       |                                    |                                |
|------------------------------|---------------|----------------|--------------------|-----------------------|------------------------------------|--------------------------------|
|                              |               |                | Control power (kW) | Calculated power (kW) | Power density (kW/m <sup>3</sup> ) | Heat flux (kW/m <sup>2</sup> ) |
| Conical test bed             |               |                |                    |                       |                                    |                                |
| COOLOCE-0 (preliminary test) | Aug 31, 2010  | 2.0            | -                  | -                     | -                                  | -                              |
| COOLOCE-1                    | Oct 21, 2010  | 1.9            | 46.2               | 40.7                  | 2326                               | -                              |
| COOLOCE-2                    | Nov 4, 2010   | 1.6            | 43.8               | 38.3                  | 2206                               | -                              |
| Cylindrical test bed         |               |                |                    |                       |                                    |                                |
| COOLOCE-3                    | May 19, 2011  | 1.1            | 19.0               | 17.3                  | 932                                | 252                            |
| COOLOCE-3R                   | Jun 17, 2011  | 1.1            | 20.4               | 18.8                  | 1001                               | 270                            |
| COOLOCE-4                    | Jun 17, 2011  | 1.6            | 23.4               | 20.6                  | 1148                               | 310                            |
|                              |               | 1.9            | 26.1               | 22.9                  | 1281                               | 346                            |
| COOLOCE-4bR                  | Jun 20, 2011  | 1.95           | 26.2               | 23.2                  | 1286                               | 347                            |
| COOLOCE-5                    | June 20, 2011 | 3.0            | 31.9               | 26.6*                 | 1565                               | 423                            |
|                              |               | 4.0            | 34.6               | 29.3                  | 1698                               | 458                            |
|                              |               | 4.95           | 37.2               | 31.0                  | 1825                               | 493                            |
|                              |               | 6.95           | 42.3               | 33.9                  | 2076                               | 560                            |
| Conical test bed             |               |                |                    |                       |                                    |                                |
| COOLOCE-6                    | Aug 22, 2011  | 1.1            | 26.0               | 23.7                  | 1488                               | -                              |
| COOLOCE-7                    | Aug 23, 2011  | 1.6            | 31.8               | 29.6                  | 1820                               | -                              |
|                              |               | 2.0            | 36.0               | 31.6                  | 2060                               | -                              |
|                              |               | 3.0            | 42.9               | 35.9                  | 2455                               | -                              |

*\*Estimate based on the heat losses of the other experiments*

Video monitoring was used in all the experiments and visual observations of boiling inside the pressure vessel were made. At all power levels with the interior of the pressure vessel at (or close to) saturation temperature, vigorous boiling was seen. In the cylindrical bed experiments, it was clearly seen that the steam rising

from the test bed is drawn towards the centre of the test bed, forming a turbulent steam column.

In the conical particle bed experiments, dryout was located near the centre of the test vessel at the height of 140 mm – 200 mm. The cylindrical particle bed also showed tendency to dryout near the centre of the test bed, in both horizontal and vertical directions. These locations slightly deviate from the theoretical incipient dryout expected for conical and cylindrical geometries but are acceptable.

An interesting observation is that the first conical test bed (COOLOCE-1 – 2) had a higher dryout power than the second test bed (COOLOCE-6 – 7) by 20 – 30%. The reason to this is not clear but it can be speculated that an unnoticed loss of heating power in the central heaters in combination with a slightly different packing of the bed might cause the difference. The dryouts observed in the second test series were very clear and even showed spreading. Thus, they have to be considered more reliable than the results of the first test series.

Pressure and power control were found to work well during the experiments, a good control of test vessel pressure and power was achieved. The exceptions to this were the COOLOCE-2 experiment which was planned to be performed at atmospheric pressure and the fluctuations of power seen in connection with overheating of the conical bed. For the COOLOCE-6 experiment, the pressure control problem was solved by removing the control valve of the steam line to reduce the flow resistance.

Overheating and damage to some of the central heaters was encountered during the conical bed experiments. After the COOLOCE-1 – 2 experiments, the condition of the heaters could be visually inspected, revealing that the outer sheaths of the heaters had been damaged in the upper parts of the conical test set-up, at the location of the expected dryout. Apparently, contact with steam at high temperatures poses a challenge to the test facility. No overheating problems were encountered with the cylindrical bed in which all the heaters have equal length, and the loading of a single heater is smaller.

## 6 Conclusions

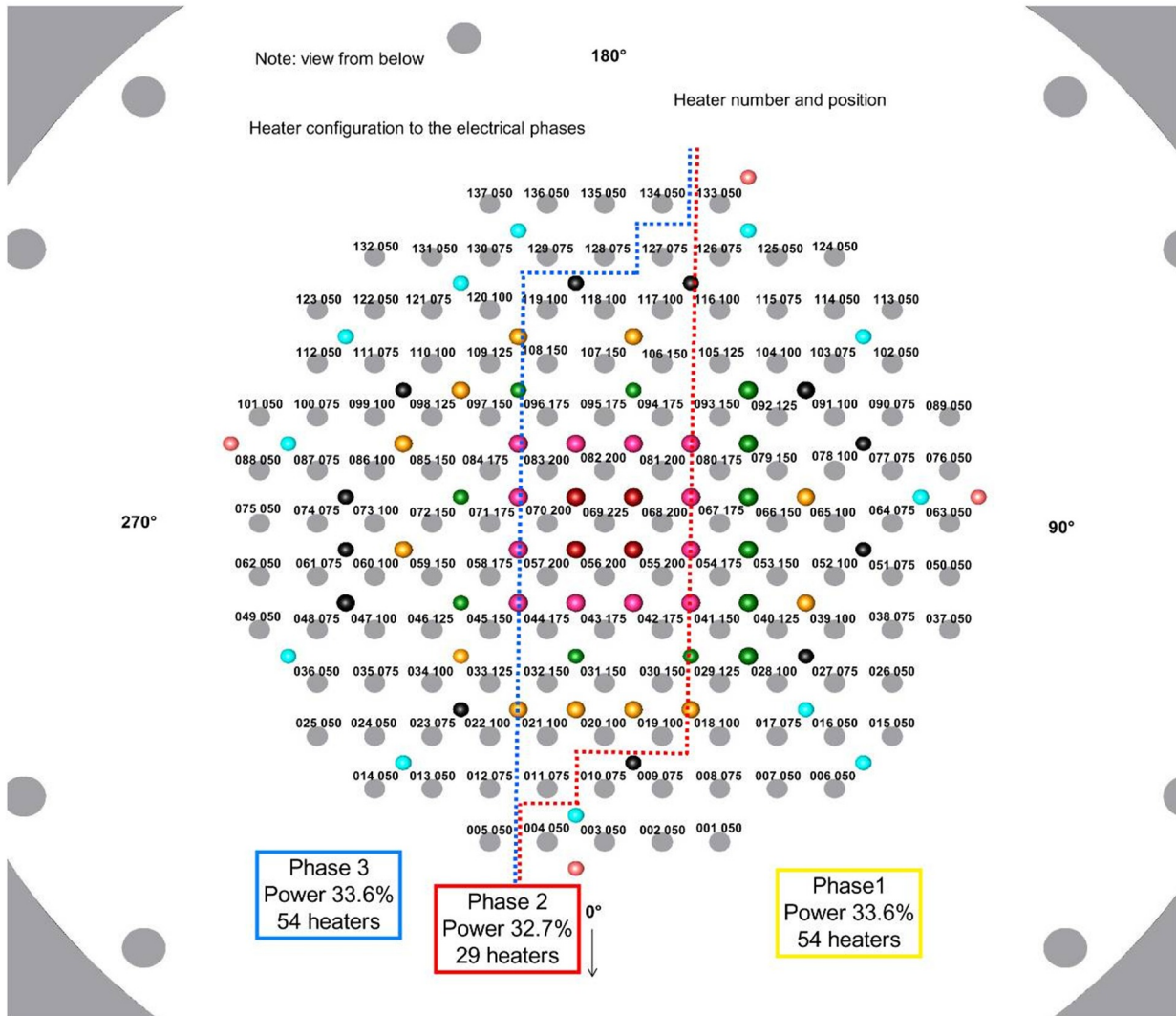
The second series of experiments with the conical particle bed has been performed. The ambient pressure in the experiments varied from atmospheric to 3 bar abs. Four measurements were performed which provide comparison data for the coolability of the cylindrical bed experiments conducted earlier. The measured dryout power varied between 26 kW and 43 kW. Based on the measurement of condensate mass flow, the power was 24 kW – 36 kW. A comparison of the dryout power (power density) of conical and cylindrical debris beds has been done. The comparison suggests that the coolability of a conical configuration is reduced by 50% compared to a cylindrical configuration of equal radius and volume. According to the present results, the cylindrical top-flooded configuration can not be considered to be the most conservative case because the incipient dryout occurs at a lower power in a conical particle than in a cylindrical particle bed. This results from the greater height of the conical configuration.

## References

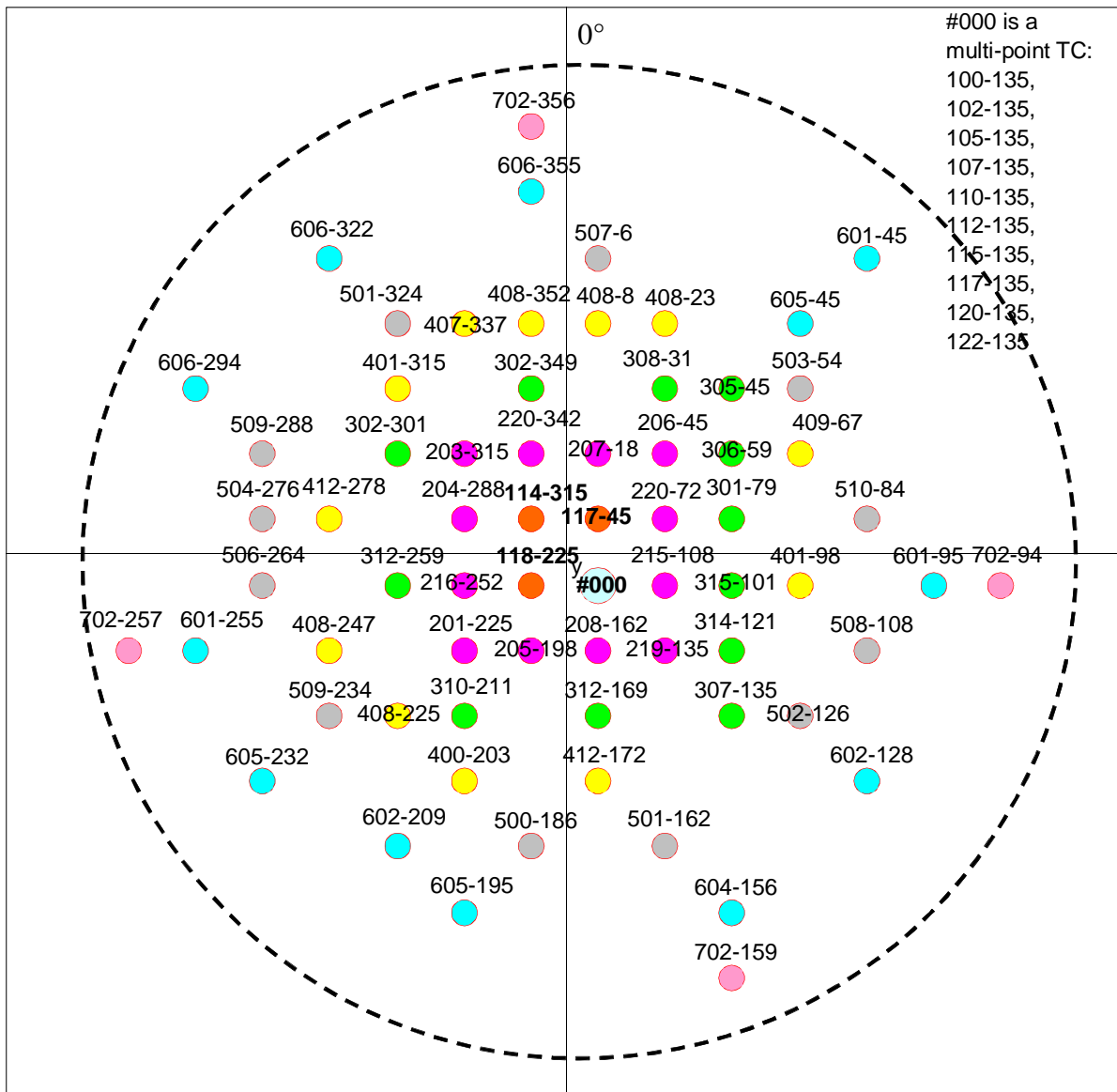
1. Takasuo, E., Kinnunen, T. Pankakoski P.H., Holmström, S. Description of the COOLOCE test facility – Conical particle bed. Research Report VTT-R-08956-10. Espoo, 2010. 18 p.
2. Takasuo, E., Kinnunen, T. Pankakoski P.H., Holmström, S. The COOLOCE-2 coolability experiment with a conical particle bed. Research Report VTT-R- 02427-11. Espoo, 2011. 15 p.
3. Takasuo, E., Kinnunen, T. Pankakoski P.H., Holmström, S. The COOLOCE coolability experiments with a cylindrical geometry: Test series 3–5. Research Report VTT-R-07099-11. Espoo, 2011. 27 p.
4. Holmström, S., Pankakoski, P., Hosio, E. STYX dry-out heat flux testing with different test bed thicknesses, Part II: homogenous and stratified tests with 600 mm and 400 mm test beds. VTT Technical Research Centre of Finland, Research Report BTUO74-051381.
5. Takasuo, E., Hovi, V., Ilvonen, M. PORFLO modelling of the coolability of porous particle beds. Research Report VTT-R-09376-10. Espoo, 2011. 41 p.
6. Takasuo, E., Holmström, S., Kinnunen, T., Pankakoski, P.H., Hosio, E., Lindholm, I. The effect of lateral flooding on the coolability of irregular core debris beds. Nuclear Engineering and Design 241 (2011), p. 1196–1205.
7. Lindholm, I., Holmström, S., Miettinen, J., Lestinen, V., Hyvärinen, J., Pankakoski, P., Sjövall, H. Dryout Heat Flux Experiments with Deep Heterogenous Particle Bed. Nuclear Engineering and Design 236 (2006), p. 2060-2074.

## APPENDIX A. Heater arrangement of the COOLOCE cone (view from below the pressure vessel bottom plate)

The positions of the heaters (colored gray) are shown relative to the positions of the thermocouples (nodes of different colors).



## APPENDIX B. Thermocouple arrangement of the COOLOCE cone (top view of the pressure vessel bottom plate)



Example of how to read the map:

### 117-45

1 – number of the zone to which the thermocouple belongs to, indicated by different colors (1 indicates the central sensors, 7 the outermost)

17 – height of the thermocouple from the bottom in cm

45 – angle between the thermocouple location and 0°

Note: Sensors that indicated dryout are in **bold**